

Magnetic, Luminescent Eu-Doped Mg–Al Layered Double Hydroxide and Its Intercalation for Ibuprofen

Jun Wang,^{*,[a]} Jideng Zhou,^[a] Zhanshuang Li,^[a] Yanchao Song,^[a] Qi Liu,^[a]
Zhaohua Jiang,^[b] and Milin Zhang^[c]

Abstract: A magnetic, luminescent Eu-doped Mg–Al layered double hydroxide with ibuprofen (IBU) intercalated in the gallery has been successfully prepared by a simple coprecipitation method. The physicochemical properties of the samples were well characterized by powder XRD, TEM, FTIR, TGA, inductively coupled plasma MS (ICP-MS), vibrating sample magnetometry (VSM), and fluorospectropho-

tometry. The results revealed that Fe₃O₄ nanoparticles are coated on the surface of layered double hydroxides and the obtained (Mg²Al_{0.95}Eu_{0.05})_{Fe}–(IBU) sample exhibits both superparamagnetic and luminescent properties,

with a saturation magnetization value of 1.86 emu g^{–1} and a strong emission band at 610 nm, respectively. Additionally, it was found that the ibuprofen loading amount is about 31 % (w/w), and the intercalated ibuprofen possesses sustained release behavior when the magnetic, luminescent composite is immersed in simulated body fluid (SBF).

Keywords: aluminum •
intercalation • luminescence •
magnesium • magnetic properties

Introduction

Layered double hydroxides (LDHs), or the so-called hydroxide-like compounds (HTlc), are a family of layered solids with structurally positively charged layers and interlayer balancing anions. The general formula of LDHs is [M^{II}_(1–x)M^{III}_x(OH)₂](A^{n–})_{x/n}·mH₂O, in which M are metal ions and A^{n–} is the interlayer anion.^[1] Organic or inorganic molecules, such as hexacyanoferrate,^[2] sulforhodamine B,^[3] porphyrins,^[4] oxacillin,^[5] and 5-fluorocytosine,^[6] can be intercalated into the gallery of the LDHs as anionic forms. In fact, the structure of LDHs looks like a brucite type with a

2D distribution of coplanar octahedra [M(OH)₆] which corresponds to the hydrolyzed layer M(OH)₂ of the brucite.^[7]

More recently, interest has been focused on using these materials in the health industry as drug supports or matrices.^[8] For example, Gordido et al. reported the immobilization of ibuprofen (IBU) and copper–ibuprofen drugs on layered double hydroxides by different methods.^[9] Drug molecules, particularly negatively charged ones, are intercalated between the positively charged layers and then released at defined target cells of tissues to affect as few healthy cells as possible.^[10,11] In general, a magnetic substrate, such as magnesium ferrite, should be chosen as the magnetic medium,^[12,13,14] then LDHs are directly coated on the magnetic medium to form a magnetic carrier system. Among the magnetic substrates, Fe₃O₄ nanoparticles, owing to their biocompatibility and excellent magnetic properties, have attracted a great deal of attention in the biomedical field, in which the magnetic properties are exploited in vitro to manipulate Fe₃O₄ nanoparticles with an external magnetic field.^[15] Li et al.^[16] reported a Fe₃O₄@SiO₂@LDH nanocomposite intercalated W₇O₂₄^{6–} anion and speculated its applications on a drug storage/release system.

A small amount of lanthanide ions can also be doped into LDHs as described in the literature.^[17–23] The methods are divided into two categories: intercalation of lanthanide complex into a LDH gallery and incorporation of lanthanide ions in a LDH lattice. Upon excitation, lanthanide ions emit

[a] Prof. J. Wang, J. Zhou, Prof. Z. Li, Y. Song, Q. Liu
College of Materials Science and Chemical Engineering
Harbin Engineering University
Harbin 150001 (P. R. China)
Fax: (+86) 451-8253-3026
E-mail: zhqw1888@sohu.com

[b] Prof. Z. Jiang
College of Chemical Engineering
Harbin Institute of Technology
Harbin 150001 (P. R. China)

[c] Prof. M. Zhang
The Key Laboratory of Superlight Materials and
Surface Technology, Ministry of Education
Harbin 150001 (P. R. China)

sharp and intense luminescence based on their f–f electronic transitions in contrast to those from organic phosphors and quantum dots.^[24,25] The combination of the luminescent properties with LDHs will open a new perspective in luminescent materials. Gunawan and Xu^[20] synthesized Tb-doped LDH intercalated with sensitizing anions and found efficient energy transfer between guest and host layers. Musesumi et al.^[21] fabricated LDH nanoparticles incorporating Tb and reported their applicability as fluorescent probes and morphology modifiers. Nevertheless, a few pieces of research on lanthanide-doped LDH intercalated with drugs have been reported. Actually, some authors^[26] have designed an Eu-doped mesoporous core-shell-structured composite material as a drug carrier, and reported that the emission intensities of Eu^{3+} in the drug system increased with the released amount of drug. So, the lanthanide-doped LDH, if intercalated with drug molecules, may be used as a luminescent label to track drug release by monitoring the luminescent intensity.

In this work, we report the synthesis and characterization of a magnetic, luminescent Mg–Al layered double hydroxide, which combines Fe_3O_4 nanoparticles, Eu^{3+} ions, and ibuprofen. To study the relationship between Fe_3O_4 and LDH particles, we fabricated magnetic Mg–Al LDHs with different amounts of Fe_3O_4 nanoparticles. The ibuprofen storage and release properties of the sample $(\text{Mg}^{2+}_{0.95}\text{Eu}_{0.05})_{\text{Fe}}(\text{IBU})$ were also investigated.

Results and Discussion

Magnetic Mg–Al LDHs: XRD patterns of magnetic LDHs with different Mg^{2+}/Fe atomic ratios are shown in Figure 1. Figure 1A–H show characteristic XRD patterns of the LDH structure,^[29] but the intensity of (003) diffraction peaks decreases with the increase of the Fe/Mg^{2+} molar ratio. It should be noted that there are no XRD patterns for Fe_3O_4 . This is because of relatively weak diffraction for magnetite and overlapping peaks at $2\theta = 35.5^\circ$ ((009) plane for LDH and (311) plane for Fe_3O_4). However, in Figure 1I, when the

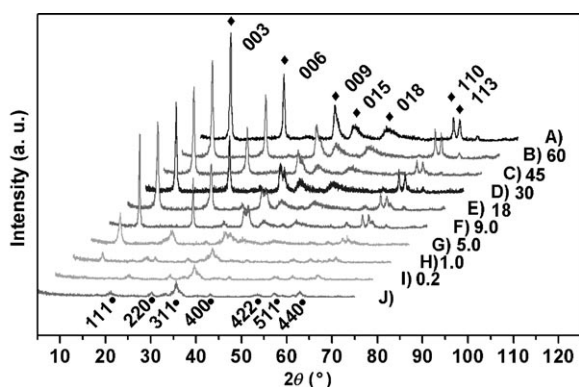


Figure 1. XRD patterns of A) $(\text{Mg}^{2+}\text{Al}_1)(\text{CO}_3^{2-})$ (♦) and magnetic $(\text{Mg}^{2+}\text{Al}_{1-x}\text{Fe}_x)(\text{CO}_3^{2-})$ with different Mg/Fe atomic ratios: B) 60, C) 45, D) 30, E) 18, F) 9, G) 5, H) 1, and I) 0.2. J) pure Fe_3O_4 (●).

Mg^{2+}/Fe molar ratio is 0.2, the characteristic diffraction peaks of the LDH structure disappear and Fe_3O_4 peaks are observed. The XRD pattern in Figure 1J was obtained from a dried Fe_3O_4 sample, whereas the Fe_3O_4 nanoparticles we used were suspended in deionized water without a drying process. In suspension, the Fe_3O_4 nanoparticles are hydrophilic and can be used for coating with LDH.^[30] During the coprecipitation process, Fe_3O_4 nanoparticles were coated on the $(\text{Mg}^{2+}\text{Al}_1)(\text{CO}_3^{2-})$ particles through hydrogen-bonding interactions (Figure 5). To support this interpretation, we prepared $(\text{Mg}^{2+}\text{Al}_1)(\text{CO}_3^{2-})$ coprecipitated with dried Fe_3O_4 powder. The results in Figure 2 demonstrated that the dried

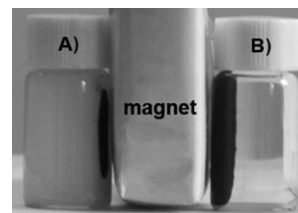


Figure 2. Photographs of $(\text{Mg}^{2+}\text{Al}_1)(\text{CO}_3^{2-})$ coprecipitated with A) dried Fe_3O_4 powder and B) Fe_3O_4 suspension.

Fe_3O_4 powder could not be coated on the surface of LDH particles. When a magnet approached the dispersion of magnetic LDH (Figure 2B), the red/brown nanohybrid particles were attracted toward the magnet within 1 min and the dispersion became clear. However, in Figure 2A, the black Fe_3O_4 powder was separated from LDH and attracted toward the magnet. A small amount of Fe_3O_4 nanoparticles coated on the LDH particle did not impede the growth of LDH crystals, but this resulted in lower crystallinity, which eventually decreased the number of the LDH gallery. Nevertheless, when all the surfaces of LDH particles were coated by Fe_3O_4 nanoparticles, the Fe_3O_4 nanoparticles began to aggregate and the LDH phase could not form. The average crystallite size of pure Fe_3O_4 calculated by using Scherrer formula^[31] is 16 nm. Considering that the Fe_3O_4 nanoparticles we used were highly dispersed in suspension, it means that the average crystallite size of Fe_3O_4 nanoparticles coated on the LDH particles is less than 16 nm and the synthesized magnetic LDH will be suitable for magnetic applications. To avoid the aggregation of Fe_3O_4 and the decrease of gallery number, the Mg^{2+}/Fe molar ratio used for fabricating magnetic, luminescent LDH and intercalating ibuprofen is 30.

The detailed morphology of the $(\text{Mg}^{2+}\text{Al}_1)(\text{CO}_3^{2-})$, magnetic $(\text{Mg}^{2+}\text{Al}_{1-x}\text{Fe}_x)(\text{CO}_3^{2-})$, and Fe_3O_4 nanoparticles are shown in Figure 3. The TEM image shown in Figure 3A indicates that nanosized $(\text{Mg}^{2+}\text{Al}_1)(\text{CO}_3^{2-})$ crystallites are mostly in the 50–100 nm size range. Figure 3B shows the electron diffraction pattern of the same sample, and the diffraction rings can be indexed as from $(\text{Mg}^{2+}\text{Al}_1)(\text{CO}_3^{2-})$, which agree with the XRD pattern shown in Figure 1A. Figure 3C–G show the morphology of magnetic $(\text{Mg}^{2+}\text{Al}_1)\text{Fe}_x$

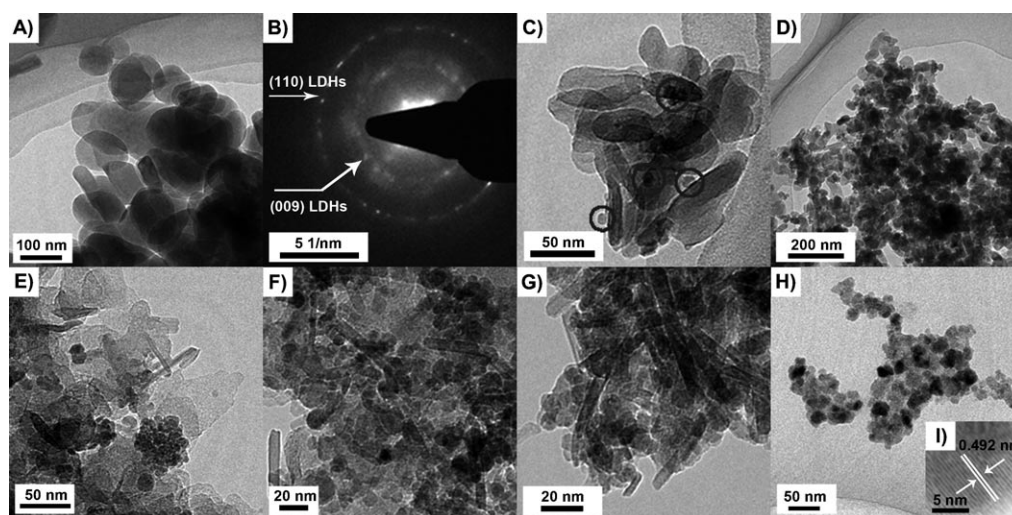


Figure 3. TEM image (A) and SAED pattern (B) of (Mg²Al₁)-(CO₃²⁻). TEM images of magnetic (Mg²Al₁)_{Fe}-(CO₃²⁻) with different Mg/Fe atomic ratios: C) 30, D) 9, E) 5, F) 1, and G) 0.2. TEM (H) and HRTEM (I) images of Fe₃O₄ nanoparticles.

(CO₃²⁻) with different Mg/Fe atomic ratios: 30, 9, 5, 1, and 0.2, respectively. The dark Fe₃O₄ nanoparticles with a 5–20 nm size range are coated on the surface of LDH, especially obviously in Figure 3C. With the increase of the Fe₃O₄ nanoparticle, it can be found that the Fe₃O₄ nanoparticles agglomerate (Figure 3E–G) more seriously, and in Figure 3E and G, platelike LDH can not be observed, instead of amorphous rodlike LDH. These phenomena in turn, can prove the weak and absent XRD patterns of LDH in Figure 1H and I. The Fe₃O₄ nanoparticles dispersed suspension was also investigated by TEM and HRTEM, as shown in Figure 3H and I. Figure 3H displays the Fe₃O₄ nanoparticle size of 5–20 nm, which approximately agrees with the calculation based on the XRD pattern (Figure 1J) and reported superparamagnetic ferrofluids (5.5–12 nm).^[32] Actually, it is hard to use large-size Fe₃O₄ particles to directly synthesize magnetic LDH, but the Fe₃O₄ core of 500 nm can be coated with a thin layer of silica, then further coated with LDH.^[16] Figure 3I exhibits a HRTEM image at higher magnification of Fe₃O₄. An interplanar distance of 0.492 nm can be determined for the (111) plane of cubic Fe₃O₄.

XRD analysis of magnetic and luminescent Mg–Al LDH intercalated with ibuprofen: Figure 4 illustrates the XRD patterns of the magnetic, luminescent (Mg²Al_{0.95}Eu_{0.05})_{Fe}-(IBU) and pristine (Mg²Al₁)-(CO₃²⁻) sample. For the (Mg²Al₁)-(CO₃²⁻) sample, the sharp and symmetric peaks demonstrate the formation of a well-crystallized LDH. It can be seen from Figure B that (Mg²Al₁)-(CO₃²⁻) has an interlayer distance value of 0.76 nm, which is similar to the value reported previously.^[33] For the (Mg²Al_{0.95}Eu_{0.05})_{Fe}-(IBU) sample, the (003) basal reflection pattern shifts to lower angle (3.6°) and the interlayer distance value is 2.45 nm. These data indicate that ibuprofen was successfully intercalated into the gallery of (Mg²Al_{0.95}Eu_{0.05})_{Fe}-LDH. In the literature,^[9,13,34] it has been reported that ibuprofen can be easily intercalated

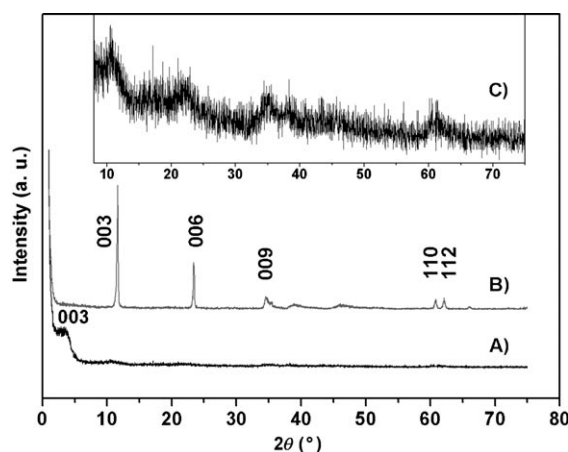


Figure 4. XRD patterns for A) (Mg²Al_{0.95}Eu_{0.05})_{Fe}-(IBU) and B) (Mg²Al₁)-(CO₃²⁻). C) High-resolution pattern of A from 5 to 75°.

into the LDH layered structure. Taking into account the brucitelike layer thickness (0.48 nm) of an individual LDH sheet,^[35,36] the gallery height corresponding to the diffraction patterns of d_{003} = 2.45 nm is 1.97 nm. According to the gallery height of (Mg²Al_{0.95}Eu_{0.05})_{Fe}-(IBU) and the length (1.03 nm) of the ibuprofen,^[37] the observed d_{003} value suggested a bilayer arrangement of the intercalated ibuprofenate anions (Figure 5). The ibuprofenate anions are perpendicular to the LDH layers by means of the interaction between –COO⁻ and –OH groups.^[9] Figure 4C is the enlargement of Figure 4B from 5 to 75°. The weak and broad peaks at 10.6° reveal that a small amount of NO₃⁻ ions still exists in the gallery of magnetic, luminescent (Mg²Al_{0.95}Eu_{0.05})_{Fe}-(IBU). In our previous work,^[38] we have confirmed that Eu³⁺ ions are incorporated in the LDH lattice (Figure 5). So, the combination of Eu³⁺ ions and Fe₃O₄ nanoparticles with LDH may offer a new perspective in drug delivery and

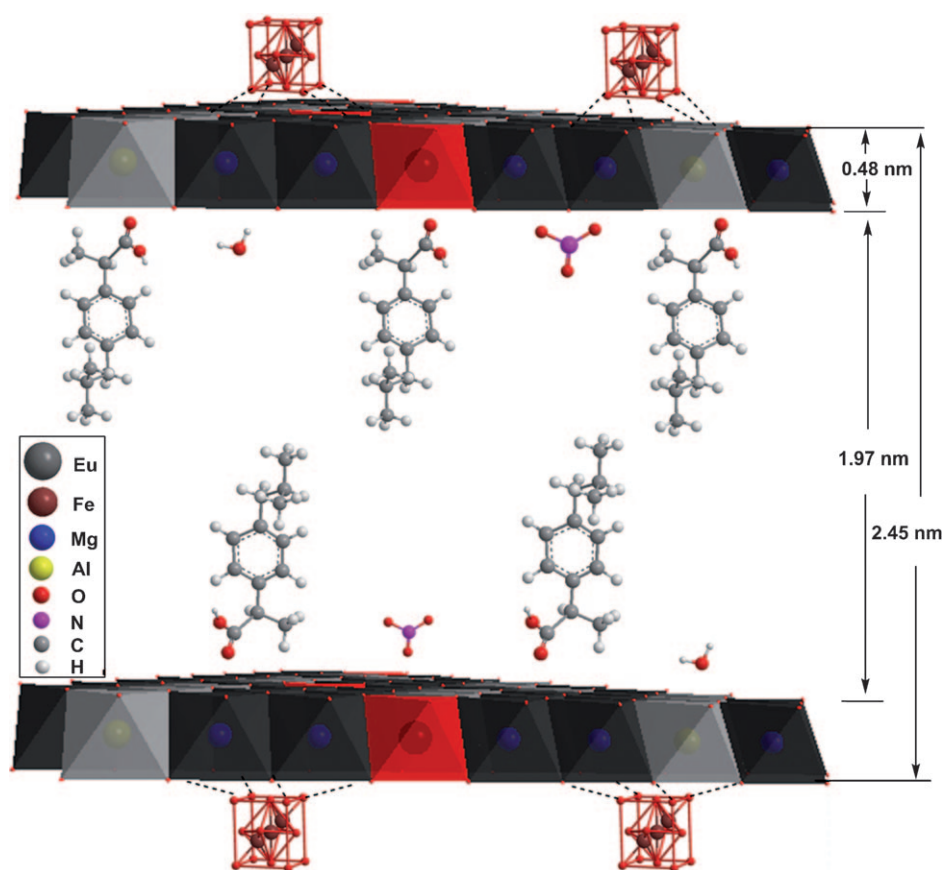


Figure 5. Schematic structural model of magnetic, luminescent $(\text{Mg}^2\text{Al}_{0.95}\text{Eu}_{0.05})_{\text{Fe}}-(\text{IBU})$.

luminescence label systems. The $\text{Al}^{3+}/\text{Eu}^{3+}$ molar ratio determined by ICP atomic emission spectroscopy is 23.

FTIR analysis: FTIR spectra of $(\text{Mg}^2\text{Al})-(\text{NO}_3^-)$, $(\text{Mg}^2\text{Al}_{0.95}\text{Eu}_{0.05})_{\text{Fe}}-(\text{IBU})$, and IBU samples are shown in Figure 6. The strong band at 1720 cm^{-1} in Figure 6C, which is attributed to the $\nu(\text{C}=\text{O})$ stretching vibration for the IBU,

disappears after intercalation, confirming that the species intercalated into the LDH layers is the anionic form of IBU. The weak bands at about 1512 , 1462 cm^{-1} in Figure 6B and 1508 , 1462 cm^{-1} in 6C are assigned to aromatic ring vibrations of IBU. The asymmetric and symmetric stretching vibrations of the $-\text{COO}^-$ group appear at 1555 and 1400 cm^{-1} , which is coherent with the reported $-\text{COO}^-$ stretching vibration (1552 and 1396 cm^{-1}).^[39] Typical alkyl stretching vibrations of IBU are observed at 2955 , 2921 , and 2868 cm^{-1} . In Figure 6A and B, the broad bands centered at around 3464 cm^{-1} are associated with the stretching vibrations of the $-\text{OH}$ groups in the LDH layers and interlayer water molecules. The water deformation vibrations are observed at 1637 cm^{-1} . The strong ν_3 stretching vibrations (1384 cm^{-1}) of interlayer nitrate ions indicates the presence of ibuprofenate and nitrate ions in the LDH gallery.^[40]

Thermal analysis: The structural stability of the compounds was examined by thermogravimetry as shown in Figure 7. Thermal decomposition of the $(\text{Mg}^2\text{Al})-(\text{CO}_3^{2-})$ sample generally proceeded through three typical steps:^[41] desorption of the physically adsorbed water molecules and partial interlayer water ($27\text{--}150^\circ\text{C}$), dehydroxylation of the layers

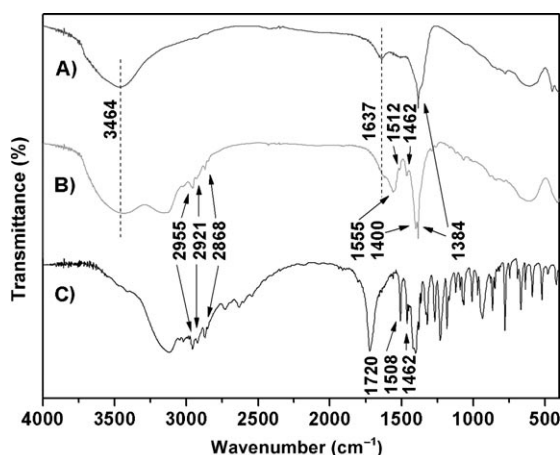


Figure 6. FTIR spectra of A) $(\text{Mg}^2\text{Al})-(\text{NO}_3^-)$, B) $(\text{Mg}^2\text{Al}_{0.95}\text{Eu}_{0.05})_{\text{Fe}}-(\text{IBU})$, and C) free IBU.

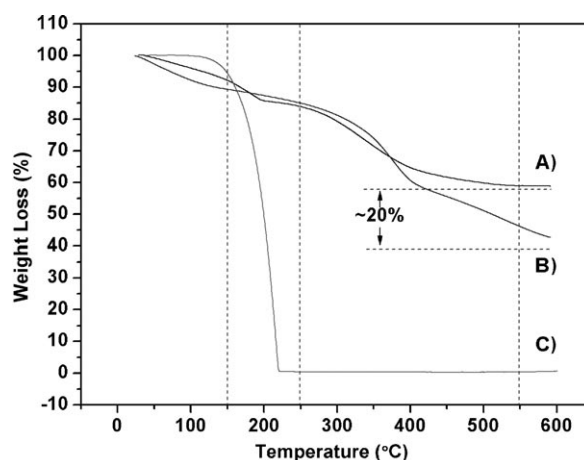


Figure 7. TG curves of A) $(\text{Mg}^2\text{Al})-(\text{CO}_3^{2-})$, B) $(\text{Mg}^2\text{Al}_{0.95}\text{Eu}_{0.05})_{\text{Fe}}-(\text{IBU})$, and C) IBU.

(150–250 °C), and decarbonylation of the interlayer carbonate ions (250–550 °C). Whereas for the $(\text{Mg}^{2+}\text{Al}_{0.95}\text{Eu}_{0.05})_{\text{Fe}}-(\text{IBU})$ sample, there is an additional and rapid mass loss within 400–600 °C; this is because the decomposition temperature of intercalated ibuprofen shifted to higher value. Compared with the decomposition temperature (around 200 °C) of pure ibuprofen, it can be concluded that the thermal stability of intercalated ibuprofen was significantly enhanced.^[12,13] From the TG curve, it is easily seen that the mass loss in the region 400–600 °C of the $(\text{Mg}^{2+}\text{Al}_{0.95}\text{Eu}_{0.05})_{\text{Fe}}-(\text{IBU})$ sample is around 20 %, which is close to the UV-measured IBU loading (31 % (w/w)). Ambrogi et al.^[39] reported $(\text{Mg}^{2+}\text{Al})-(\text{IBU})$ with ibuprofen loading of 50 % (w/w) and Gordijo et al.^[9] obtained 30 % (w/w) of ibuprofen intercalated in $(\text{Mg}^{3+}\text{Al})-\text{LDH}$. The different IBU content may be due to the following reasons: 1) $(\text{Mg}^{2+}\text{Al})-\text{LDH}$ exhibits higher charge density relative to $(\text{Mg}^{3+}\text{Al})-\text{LDH}$ and 2) the Fe_3O_4 nanoparticles covered on the LDH platelet decreased the number of the LDH gallery.

Morphology analysis: The morphological features of the $(\text{Mg}^{2+}\text{Al}_{0.95}\text{Eu}_{0.05})_{\text{Fe}}-(\text{IBU})$ observed by using TEM are displayed in Figure 8. Figure 8A indicates the loading of IBU

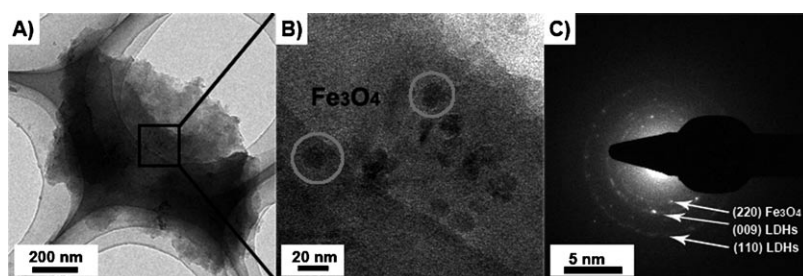


Figure 8. TEM images (A and B) and SAED pattern (C) of magnetic and luminescent $(\text{Mg}^{2+}\text{Al}_{0.95}\text{Eu}_{0.05})_{\text{Fe}}-(\text{IBU})$.

on LDH induced the obvious aggregation. This aggregation can be found in reported ibuprofen^[39] and other molecule^[42] intercalated LDHs. In Figure 8B, it is clearly shown that Fe_3O_4 nanoparticles are dispersed in the magnetic and luminescent LDH hybrid. The corresponding SAED pattern is shown in Figure 8C, the diffraction rings from the inner to outer are indexed as from (220) Fe_3O_4 , (009) LDHs, and (110) LDHs.

Drug-release properties: To study the ibuprofen-release properties from $(\text{Mg}^{2+}\text{Al}_{0.95}\text{Eu}_{0.05})_{\text{Fe}}-(\text{IBU})$, the cumulative drug-release profiles versus release time in simulated body fluid (SBF) are shown in Figure 9. It can be seen that the physical mixture (Figure 9B) releases ibuprofen quickly, and the release is completed within 1.5 h. By comparison, the release rate of $(\text{Mg}^{2+}\text{Al}_{0.95}\text{Eu}_{0.05})_{\text{Fe}}-(\text{IBU})$ (Figure 9A) is obviously lower than that of physical mixture. In Figure 9A, a rapid release within the initial 1.5 h is followed by a sustained release of the remaining ibuprofen, which is similar to the release results of other drugs^[43,44] from LDHs. The

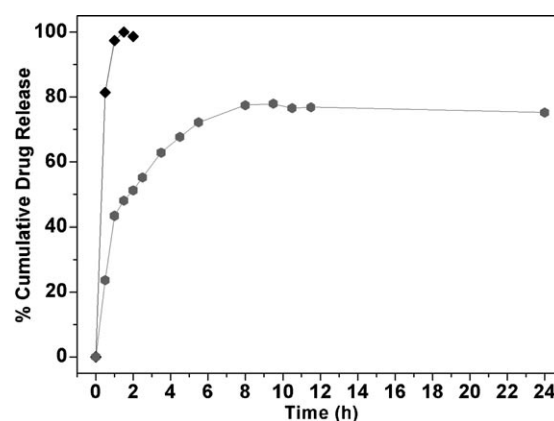


Figure 9. Cumulative drug-release curves of A) $(\text{Mg}^{2+}\text{Al}_{0.95}\text{Eu}_{0.05})_{\text{Fe}}-(\text{IBU})$ (●) and B) a physical mixture of IBU and $(\text{Mg}^{2+}\text{Al})-(\text{CO}_3^{2-})$ (◆).

difference is probably due to the ibuprofen release mechanism. For the physical mixture, the mechanism is through desorption, whereas for $(\text{Mg}^{2+}\text{Al}_{0.95}\text{Eu}_{0.05})_{\text{Fe}}-(\text{IBU})$ it is through ion-exchange^[45,46,47] between interlayer ibuprofenate and the Cl^- , HCO_3^- , or HPO_4^{2-} ions in SBF. However, the release amount is only 78 % (w/w) and no release can be observed beyond 10 h. Our results differ from that reported by Ambrogi et al.^[39] who have applied phosphate buffer solution (PBS) as the release medium. So, we believe that the ion-exchange in SBF may reach an equilibrium, which leads to the suspension of IBU release after 10 h. These release profiles indicate the possibility of $(\text{Mg}^{2+}\text{Al}_{0.95}\text{Eu}_{0.05})_{\text{Fe}}-\text{LDH}$ being used as a drug carrier in a sustained release system.

Luminescent properties: The luminescent properties of the sample $(\text{Mg}^{2+}\text{Al}_{0.95}\text{Eu}_{0.05})_{\text{Fe}}-(\text{IBU})$ were characterized by excitation and emission spectra, as shown in Figure 10. The excitation spectrum was monitored by the $\text{Eu}^{3+}{}^5\text{D}_0-{}^7\text{F}_2$ transition at 610 nm. The broad band with a maximum at 269 nm arises from excitation of the π electrons of the aromatic ring^[17,19] in the ibuprofenate ion. The bands at short wavelengths (237 and 243 nm) could be partially contributed by the LDH lattice.^[20] The weak peak at 398 nm corresponds to the direct excitation of the Eu^{3+} ground state into a higher level of the 4f-manifold, which can be ascribed to ${}^7\text{F}_0-{}^5\text{L}_6$.^[48] The relatively lower intensity of Eu^{3+} f–f transition lines indicates that the excitation of Eu^{3+} mainly results from the energy transfer from the LDH lattice and ibuprofen to Eu^{3+} . The emission spectrum (Figure 10B) was obtained by the excitation at 269 nm. It can be seen that the sample $(\text{Mg}^{2+}\text{Al}_{0.95}\text{Eu}_{0.05})_{\text{Fe}}-(\text{IBU})$ exhibits four characteristic emission lines, which are ascribed to ${}^5\text{D}_0-{}^7\text{F}_J$ ($J=1, 2, 3, 4$) transitions of the Eu^{3+} ion, respectively.^[49] Thus, the introduction

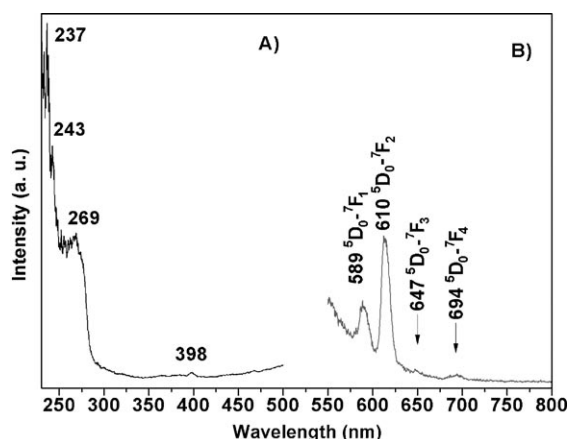


Figure 10. Excitation (A, emission wavelength is 610 nm) and emission spectra (B, excitation wavelength is 269 nm).

of Fe_3O_4 may not affect the luminescent properties of the resulting composite. In other words, the route of coating Fe_3O_4 nanoparticles on the surface of LDH particle, to some extent, could avoid the quenching interaction^[50] between the Eu^{3+} ions and Fe_3O_4 nanoparticles. Such a phenomenon has already been observed for $\text{Y}_2\text{O}_3/\text{Tb}$ nanorods on the surface of iron oxide/silica core-shell nanostructures.^[51] But the quenching effect of intercalated ibuprofenate ions on Eu^{3+} still exists. As a result, the quenching effect is weakened with the ibuprofen release amount and subsequently the luminescent intensity of Eu^{3+} ions is enhanced. It is the correlation between the luminescence intensity and drug release amount that make the composite possible as a probe for monitoring the drug release.^[26]

Magnetic properties: The magnetic hysteresis curves of $(\text{Mg}^{2+}\text{Al}_{0.95}\text{Eu}_{0.05})\text{Fe}-(\text{IBU})$ and pure Fe_3O_4 (insert) were measured at room temperature, as demonstrated in Figure 11. The negligible coercivity or remanence indicates that both

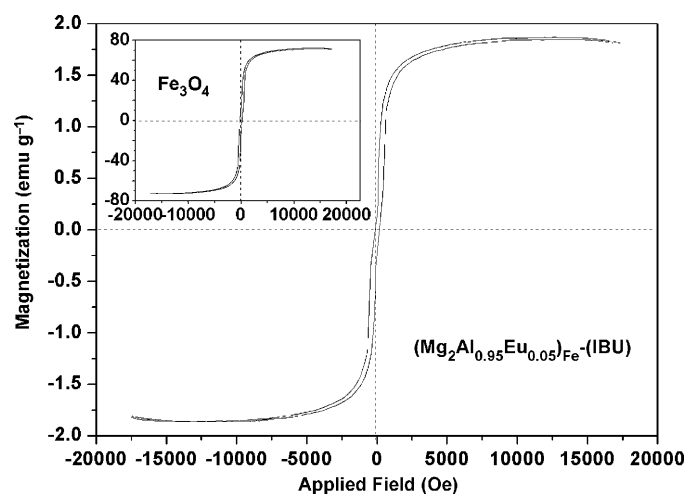


Figure 11. Magnetic hysteresis curves of $(\text{Mg}^{2+}\text{Al}_{0.95}\text{Eu}_{0.05})\text{Fe}-(\text{IBU})$ and Fe_3O_4 (insert) at room temperature.

of them exhibit superparamagnetic behavior. The saturation magnetizations of sample $(\text{Mg}^{2+}\text{Al}_{0.95}\text{Eu}_{0.05})\text{Fe}-(\text{IBU})$ is 1.86 emu g^{-1} , which is lower than that of pure Fe_3O_4 (73 emu g^{-1}), but enough for common bioseparation.^[25] So, the magnetic and luminescent LDH can quickly respond to the external magnetic field and quickly redisperse once the external magnetic field is removed.^[52]

Conclusion

We have synthesized the magnetic, luminescent Eu-doped Mg–Al LDH intercalated with ibuprofen, by a simple wet chemical method. This inorganic/organic hybrid material shows both superparamagnetic and luminescent properties at room temperature. Detailed characterizations confirmed that Fe_3O_4 nanoparticles coated on the LDH particles and the quenching effect between the Fe_3O_4 nanoparticles and Eu^{3+} ions is very weak. The storage amount of ibuprofen determined by UV/Vis spectrophotometry was 31 % (w/w). The results of in vitro drug release in SBF revealed that the magnetic, luminescent LDHs have potential applications as targeted drug delivery systems. Moreover, the incorporation of rare-earth ions into the LDH structure may offer new possibilities in tracing the intercalated drug amount by monitoring its luminescent properties.

Experimental Section

Materials: Eu_2O_3 was kindly provided to us by the Changchun Institute of Applied Chemistry Chinese Academy of Sciences. Ibuprofen was purchased from the General Pharmaceutical Factory of Harbin Pharmaceutical Group. Other inorganic reagents were purchased from Tianjin Kermel Chemical Reagents Development Center. All chemicals were of analytical grade and were used without further purification.

Preparation of $\text{Eu}(\text{NO}_3)_3$ solution: White Eu_2O_3 powder (0.88 g, 2.5 mmol) was dissolved in excess concentrated nitric acid. After adding a known volume of water to the formed solution, excessive levels of nitric acid were removed by the distillation method. The concentration of obtained $\text{Eu}(\text{NO}_3)_3$ solution was 0.02 mol L^{-1} .

Preparation of magnetic substrates: Magnetic Fe_3O_4 nanoparticles were prepared by the coprecipitation method. With stirring at 45°C , a mixed salt solution containing $\text{Fe}_2(\text{SO}_4)_3$ (4.00 g, 10.0 mmol), FeSO_4 (2.78 g, 10.0 mmol), and $\text{NH}_3\cdot\text{H}_2\text{O}$ (26 wt. %) were added dropwise together at a constant pH value of 11. The formed suspension was isolated by a magnet and washed several times with deionized water until the pH was neutral. The obtained Fe_3O_4 nanoparticles were preserved as a suspension and used as a well-shaken homogenous system. The concentration of the element iron was 0.05 mol L^{-1} .

Synthesis of magnetic layered double hydroxides: Carbonate-containing magnetic LDHs with a $\text{Mg}^{2+}/\text{Al}^{3+}$ molar ratio of 2 (hereafter $(\text{Mg}^{2+}\text{Al})_{\text{Fe}}-(\text{CO}_3^{2-})$) were prepared by the coprecipitation method. An aqueous solution (90 mL) containing $\text{Mg}(\text{NO}_3)_2\cdot 6\text{H}_2\text{O}$ (6.15 g, 24.0 mmol) and $\text{Al}(\text{NO}_3)_3\cdot 9\text{H}_2\text{O}$ (4.51 g, 12.0 mmol) was added dropwise to an aqueous solution (90 mL) containing Na_2CO_3 and magnetic substrates, with an $\text{Al}^{3+}/\text{CO}_3^{2-}$ molar ratio equal to 1 and a Mg^{2+}/Fe molar ratio equal to 30 with vigorous stirring. During the synthesis, an aqueous solution of NaOH was added dropwise at 80°C with vigorous stirring to adjust the pH to 10. The resulting solid products were separated by a magnet, washed with deionized water, and dried at 80°C for 24 h. The above procedure was repeated, altering the amount of magnetic sub-

strates added while keeping other reaction conditions constant to give a series of magnetic LDHs.

Synthesis of magnetic, luminescent layered double hydroxides intercalated with ibuprofen: The ibuprofen intercalated magnetic, luminescent Eu-doped Mg–Al LDH was synthesized by the following procedure: Under a N₂ atmosphere, a mixed salt solution containing Mg(NO₃)₂·6H₂O (6.15 g, 24.0 mmol), Al(NO₃)₃·9H₂O (4.28 g, 11.5 mmol), and Eu(NO₃)₃ (0.5 mmol) was added dropwise to an aqueous solution (100 mL) containing ibuprofen (2.48 g, 12.0 mmol) and magnetic substrates (16 mL) with a Mg²⁺/Fe molar ratio equal to 30 under vigorous stirring. The pH value of the system was adjusted by a NaOH solution. The precipitate was aged for 12 h in the mother solution at 80 °C and then isolated by a magnet and washed with deionized water. The resulting solid products were dried at 80 °C for 24 h in a vacuum oven and abbreviated here as (Mg²⁺Al_{0.95}Eu_{0.05})_{Fe}-(IBU).

Calibration graph for ibuprofen determination: Calibration graph of absorbance versus concentration of the free ibuprofen was plotted by monitoring the ibuprofen typical UV absorption band at 264 nm^[27] for a concentration range of 20–400 µg mL⁻¹ of the drug in the mixture of 1:1 (v/v) ethanol/HCl (1 mol L⁻¹). The amount of ibuprofen intercalated in the LDH gallery was determined by comparing the absorbance of a sample solution to the data from the calibration curve.

In vitro drug release: The release of ibuprofen in vitro experiment was performed as follows: The sample (0.08 g) was immersed in SBF (200 mL) with mild shaking at 150 rpm and the immersing temperature was kept at 37 °C. The SBF solution had a similar composition and concentration (Na⁺: 142, K⁺: 5.0, Mg²⁺: 1.5, Ca²⁺: 2.5, Cl⁻: 147.8, HCO₃⁻: 4.2, HPO₄²⁻: 1.0, and SO₄²⁻: 0.5 mmol L⁻¹; pH 7.4)^[26,28] to that of human plasma. At a given time, the sample was captured by using a magnet and an aliquot of the solution (5 mL) was removed for measurement of released ibuprofen into the solution and immediately replaced by an equal volume of SBF to keep the volume constant. The content of ibuprofen in each aliquot was measured by the absorbance at 264 nm by using a UV/Vis spectrophotometer.

Characterizations: Powder XRD patterns of the solid products were obtained in the 2θ range of 1–75° by using a Rigaku D/max-III B diffractometer with Cu Kα radiation (λ = 1.54178 Å). Morphology was characterized by using TEM (PHILIPS CM 200 FEG, 160 kV). FTIR spectra were recorded with an AVATAR 360 FTIR spectrophotometer by using a standard KBr pellet technique. TGA was carried out by heating the dry powder samples at a rate of 10 °C min⁻¹ in NEZSCH STA 409 PC. Magnetic hysteresis loops of samples were measured by a JDM-13 vibrating sample magnetometer (VSM) at room temperature. The fluorescence spectra of samples were characterized by using a PerkinElmer LS 55 fluorospectrophotometer under identical conditions with an excitation wavelength of 610 nm and emission spectra in the range of 500–800 nm. The width of the excitation and emission slit is 15 and 20 nm, respectively. The emission spectra were measured by exciting the samples with a 150 W Xe lamp. Elemental analyses were performed by ICP atomic emission spectroscopy by using solutions prepared by dissolving the samples in concentrated HNO₃. The absorbance of ibuprofen was measured by UV/Vis spectroscopy (UV-1601).

Acknowledgements

Financial support from the Key Technology R&D program of Heilongjiang Province (no. TB06A05), the Science Fund for Young Scholars of Harbin City (no. 2008RFQXG028), and Fundamental Research Funds for the Central University (no. HEUCF101010) are greatly acknowledged.

- [1] S. P. Gao, T. H. Lu, S. P. Li, H. Zhong, *Colloids Surf. A* **2009**, *351*, 26–29.
- [2] H. S. Panda, R. Srivastava, D. Bahadur, *J. Phys. Chem. C* **2009**, *113*, 9560–9567.

- [3] D. Yan, J. Lu, M. Wei, D. G. Evans, X. Duan, *J. Phys. Chem. B* **2009**, *113*, 1381–1388.
- [4] K. Lang, P. Bezdička, J. Bourdelande, J. Hernando, I. Jirka, E. Káfuňková, *Chem. Mater.* **2007**, *19*, 3822–3829.
- [5] G. Carja, Y. Kameshima, G. Ciobanu, H. Chiriac, K. Okada, *Micron* **2009**, *40*, 147–150.
- [6] C. X. Liu, W. G. Hou, L. F. Li, Y. Li, S. J. Liu, *J. Solid State Chem.* **2008**, *181*, 1792–1797.
- [7] P. Beaudot, M. E. D. Roy, J. P. Besse, *Chem. Mater.* **2004**, *16*, 935–945.
- [8] J. H. Choy, S. J. Choi, J. M. Oh, T. Park, *Appl. Clay Sci.* **2007**, *36*, 122–132.
- [9] C. R. Gordijo, C. A. S. Barbosa, M. D. C. Ferreira, V. R. L. Constavtino, D. D. O. Silva, *J. Pharm. Sci.* **2005**, *94*, 1135–1148.
- [10] S. Chen, Y. Li, C. Guo, J. Wang, J. Ma, X. Liang, *Langmuir* **2007**, *23*, 12669–12676.
- [11] J. Wang, Q. Liu, G. Zhang, Z. Li, P. Yang, X. Jing, *Solid State Sci.* **2009**, *11*, 1597–1609.
- [12] H. Zhang, K. Zou, H. Sun, X. Duan, *J. Solid State Chem.* **2005**, *178*, 3485–3493.
- [13] A. N. Ay, B. Zümreoglu-Karan, A. Temel, V. Rives, *Inorg. Chem.* **2009**, *48*, 8871–8877.
- [14] H. Zhang, D. Pan, X. Duan, *J. Phys. Chem. C* **2009**, *113*, 12140–12148.
- [15] P. Majewski, B. Thierry, *Crit. Rev. Solid State Mater. Sci.* **2007**, *32*, 203–215.
- [16] L. Li, Y. Feng, Y. Li, W. Zhao, J. Shi, *Angew. Chem.* **2009**, *121*, 6002–6006; *Angew. Chem. Int. Ed.* **2009**, *48*, 5888–5892.
- [17] N. G. Zhuravleva, A. A. Eliseev, A. V. Lukashin, U. Kynast, A. Y. D. Tret'yakov, *Dokl. Chem.* **2004**, *396*, 87–91.
- [18] C. Li, G. Wang, D. G. Evans, X. Duan, *J. Solid State Chem.* **2004**, *177*, 4569–4575.
- [19] Z. Chang, D. Evans, X. Duan, P. Boutinaud, M. D. Roy, C. Forano, *J. Phys. Chem. Solids* **2006**, *67*, 1054–1057.
- [20] P. Gunawan, R. Xu, *J. Phys. Chem. C* **2009**, *113*, 17206–17214.
- [21] A. W. Musumeci, Z. P. Xu, S. V. Smith, R. F. Minchin, D. J. Martin, *J. Nanopart. Res.* **2010**, *12*, 111–120.
- [22] J. M. Fernández, C. Barriga, M. A. Ulibarri, F. M. Labajos, V. Rives, *Chem. Mater.* **1997**, *9*, 312–318.
- [23] T. Stumpf, H. Curtius, C. Walther, K. Dardenne, K. Ufer, T. F. Nel, *Environ. Sci. Technol.* **2007**, *41*, 3186–3191.
- [24] G. A. Crosby, R. E. Whan, R. M. Alire, *J. Chem. Phys.* **1961**, *34*, 743–748.
- [25] H. Lu, G. Yi, S. Zhao, D. Chen, L. H. Guo, J. Cheng, *J. Mater. Chem.* **2004**, *14*, 1336–1341.
- [26] P. Yang, Z. Quan, Z. Hou, C. Li, X. Kang, Z. Cheng, *Biomaterials* **2009**, *30*, 4786–4795.
- [27] M. Redpath, C. M. G. Marques, C. Dibden, A. Waddon, R. Lalla, S. MacNeil, *Br. J. Dermatol.* **2009**, *161*, 25–33.
- [28] M. Vallet-Regí, J. Pérez-Pariente, I. Izquierdo-Barba, A. J. Salinas, *Chem. Mater.* **2000**, *12*, 3770–3775.
- [29] K. H. Goh, T. T. Lim, Z. Dong, *Water Res.* **2008**, *42*, 1343–1368.
- [30] J. L. Zhang, R. S. Srivastava, R. D. K. Misra, *Langmuir* **2007**, *23*, 6342–6351.
- [31] A. W. Burton, K. Ong, T. Rea, I. Y. Chan, *Microporous Mesoporous Mater.* **2009**, *117*, 75–90.
- [32] M. F. Casula, P. Floris, C. Innocenti, A. Lascialfari, M. Marinone, M. Corti, *Chem. Mater.* **2010**, *22*, 1739–1748.
- [33] B. Li, J. He, *J. Phys. Chem. C* **2008**, *112*, 10909–10917.
- [34] K. L. Dagnon, S. Ambadapadi, A. Shaito, S. M. Ogbomo, V. DeLeon, T. D. Golden, *J. Appl. Polym. Sci.* **2009**, *113*, 1905–1915.
- [35] S. Bégu, A. Aubert-Pouessel, R. Pollex, E. Leitmanova, D. A. Lerner, J. M. Devoisselle, *Chem. Mater.* **2009**, *21*, 2679–2687.
- [36] H. Chai, Y. Lin, D. G. Evans, D. Li, *Ind. Eng. Chem. Res.* **2008**, *47*, 2855–2860.
- [37] M. Vallet-Regí, A. Rámila, R. P. D. Real, J. Pérez-Pariente, *Chem. Mater.* **2001**, *13*, 308–311.
- [38] J. Wang, J. Zhou, Z. Li, Q. Liu, P. Yang, X. Jing, *Mater. Res. Bull.* **2010**, *45*, 645–650.

- [39] V. Ambroggi, G. Fardella, G. Grandolini, L. Perioli, *Int. J. Pharm.* **2001**, *220*, 23–32.
- [40] S. V. Prasanna, P. V. Kamath, *Ind. Eng. Chem. Res.* **2009**, *48*, 6315–6320.
- [41] H. Zhang, S. H. Guo, K. Zou, X. Duan, *Mater. Res. Bull.* **2009**, *44*, 1062–1069.
- [42] D. P. Qiu, W. G. Hou, *Colloids Surf. A* **2009**, *336*, 12–17.
- [43] M. Wei, M. Pu, J. Guo, J. B. Han, F. Li, J. He, *Chem. Mater.* **2008**, *20*, 5169–5180.
- [44] H. S. Panda, R. Srivastava, D. Bahadur, *J. Phys. Chem. B* **2009**, *113*, 15090–15100.
- [45] V. Ambroggi, L. Perioli, V. Ciarnelli, M. Nocchetti, C. Rossi, *Eur. J. Pharm. Biopharm.* **2009**, *73*, 285–291.
- [46] Z. Wang, E. B. Wang, L. Gao, L. Xu, *J. Solid State Chem.* **2005**, *178*, 736–741.
- [47] W. Z. Li, J. Lu, J. S. Chen, G. D. Li, Y. S. Jiang, L. S. Lian, *J. Chem. Technol. Biotechnol.* **2006**, *81*, 89–93.
- [48] C. Li, Z. W. Quan, J. Yang, P. Yang, J. Lin, *Inorg. Chem.* **2007**, *46*, 6329–6337.
- [49] Z. L. Wang, Y. Ma, R. Zhang, A. Peng, Q. Liao, Z. Cao, *Adv. Mater.* **2009**, *21*, 1737–1741.
- [50] J. J. Brege, C. Gallaway, A. R. Barron, *J. Phys. Chem. C* **2007**, *111*, 17812–17820.
- [51] Y. Zhang, S. Pan, X. Teng, Y. Luo, G. Li, *J. Phys. Chem. C* **2008**, *112*, 9623–9626.
- [52] J. Feng, S. Y. Song, R. P. Deng, W. Q. Fan, H. J. Zhang, *Langmuir* **2010**, *26*, 3596–3600.

Received: March 8, 2010

Revised: June 30, 2010

Published online: October 29, 2010